

Strain driven charge-ordered state in $\text{La}_{0.67}\text{Ca}_{0.33}\text{MnO}_3$

Amlan Biswas, M. Rajeswari, R. C. Srivastava, T. Venkatesan, and R. L. Greene
Center for Superconductivity Research, University of Maryland, College Park, MD-20742

Q. Lu and A. L. de Lozanne
Department of Physics, University of Texas, Austin, TX-78712

A. J. Millis
Center for Materials Theory, Department of Physics and Astronomy, Rutgers University, Piscataway, NJ-08854
(October 29, 2018)

We present evidence for the coexistence of ferromagnetic metallic and charge ordered insulating phases in strained thin films of $\text{La}_{0.67}\text{Ca}_{0.33}\text{MnO}_3$ at low temperatures. Such a phase separated state is confirmed using low temperature magnetic force microscopy and magnetotransport measurements. This phase separated state is not observed in the bulk form of this compound and is caused by the structural inhomogeneities due to the non-uniform distribution of strain in the film. The strain weakens the low temperature ferromagnetic metallic state and a charge ordered insulator is formed at the high strain regions. The slow dynamics of the transport properties of the mixed phase is illustrated by measurements of the long time scale relaxation of the electrical resistance.

I. INTRODUCTION

The hole-doped perovskite manganites are of great current interest for the range of novel properties they display and for the possibility they offer of new devices. Thin films are important both for fundamental studies and for potential applications, but the relation between film properties and those of bulk materials is not well understood. In this paper we show that strain associated with a lattice mismatched substrate can cause new electronic behavior, not found in bulk materials of the same chemical composition. In hole-doped manganites with the chemical formula $\text{RE}_{1-x}\text{AE}_x\text{MnO}_3$ (RE is a trivalent rare earth ion and AE is divalent alkaline earth ion) a complex interplay of the charge, lattice, spin and orbital degrees of freedom leads to various novel properties. Of special interest are the metal-insulator (MI) transition at the ferromagnetic Curie temperature (T_C) and the phenomenon of charge ordering. These transitions occur at a wide range of temperatures depending on the compound i.e. factors like the hole doping concentration x , the average A-site cation radius $\langle r_A \rangle$ (A-site refers to the ABO_3 perovskite structure, where the A-site is occupied by the RE or AE ion and the B-site is occupied by the Mn ions), and the variance in the radii of the A-site cations $\langle \sigma_A \rangle$ all of which effectively perturb one or more of the degrees of freedom mentioned above [1,2]. Introducing such perturbations profoundly affects the stability of the ground state and gives more insight about the energy considerations for these transitions.

Beyond the pure phase behavior, the observation of electronic phase separation in these materials has generated considerable interest [3,4]. It has been shown that for a wide range of temperatures there is a coexistence of ferromagnetic metallic (FMM) and charge ordered insulating (COI) phases in some of these materials. This

phenomenon has been observed for different values of x , $\langle r_A \rangle$, and $\langle \sigma_A \rangle$. The low temperature FMM state for $x \sim 0.3$ and the phenomenon of charge ordering (CO) for $x = 0.5$ is observed in a variety of manganite systems and has been studied extensively, both experimentally and theoretically. However, as $\langle r_A \rangle$ is reduced below about 1.18 Å, the FMM state disappears and the paramagnetic insulating state goes directly to the charge ordered insulating state at low temperatures as observed in the compound $\text{Pr}_{1-x}\text{Ca}_x\text{MnO}_3$. This CO state can be made progressively unstable by replacing the Pr ion with the larger La ion. A focus of particular attention is the compound $(\text{La}_{1-y}\text{Pr}_y)_{5/8}\text{Ca}_{3/8}\text{MnO}_3$. For $y=1$, the COI phase is observed and for $y=0$ the FMM phase is observed, at low temperatures. For intermediate values of y , multiphase behavior is observed at low temperatures characterized by the history dependence and slow time relaxation of the resistivity.

In these compounds the COI and the FMM states have very similar energies, resulting in the two-phase coexistence of FMM and COI regions [3]. The similarity of the energies of the FMM and COI phases leads to a sensitive balance between the FMM and COI regions, which can be tilted in favor of the FMM phase by the application of a magnetic field or external hydrostatic pressure and towards the COI phase by an increase in the structural distortion away from the ideal cubic perovskite lattice. The structural distortion can be increased by applying internal pressure by the substitution of smaller ions at the A-site or by applying anisotropic stress [1,5,6].

These observations suggest that interesting phenomena may be observed in highly strained thin films of manganites. In a previous work we have shown the existence of a strain-induced insulating state in biaxially strained films of $\text{La}_{0.67}\text{Ca}_{0.33}\text{MnO}_3$ (LCMO) and we claimed that this was caused by the non-uniform distribution of the

strain which leads to a possible two-phase behavior [6]. Here, we present, detailed studies of the magnetic structure, using low temperature magnetic force microscopy (MFM), and the magnetotransport properties of such biaxially strained films of LCMO that lend strong support to our claims. While in its bulk form, LCMO is a ferromagnetic metal at low temperature with a pseudo-cubic lattice structure, we show that the biaxial strain results in a distortion of the lattice structure of LCMO. This distortion makes the low temperature FMM state unstable and a CO state develops instead. Furthermore, we show that the strain is non-uniformly distributed, which leads to a two-phase coexistence of FMM and COI regions very similar to that exhibited by $(\text{La}_{1-y}\text{Pr}_y)_{5/8}\text{Ca}_{3/8}\text{MnO}_3$. This is confirmed using low temperature MFM measurements. We present the various novel properties of this strain driven two-phase state and discuss the implications on the properties of hole-doped manganites.

II. EXPERIMENTAL DETAILS

Thin films of $\text{La}_{0.67}\text{Ca}_{0.33}\text{MnO}_3$ (LCMO), 150 Å in thickness, were grown on (001) LaAlO_3 (LAO) and (110) NdGaO_3 (NGO) substrates by pulsed laser deposition (PLD). There is a compressive lattice mismatch strain of $\sim 2\%$ for a film of LCMO on LAO while on NGO this strain is negligible (less than 0.1 %). Details of the film growth are given in [6]. The resistivities were measured by the conventional four-probe method and the DC magnetization was measured using a SQUID magnetometer. The lattice parameters were measured using a Siemens D5000 diffractometer equipped with a four circle goniometer. The nanostructure of the films were measured using a Nanoscope III AFM operated in the tapping mode.

The low temperature MFM has been described in detail previously [7,8]. It is a frequency-modulated MFM that measures the magnetic force gradient $F'(x,y)$ distribution on a sample. Briefly, a positive feedback loop forces a piezo-resistive cantilever to vibrate at its resonant frequency, ω_0 . A magnetic tip with iron coating is located at the free end of the cantilever. During an imaging process, the non-uniform magnetic stray field from the sample will cause this ω_0 to change. A second feedback system prevents ω_0 from shifting by adjusting the tip-sample distance. The output of this feedback system is used to construct an image of constant force gradient. This low temperature MFM has been used to study a variety of materials [7–11].

The cantilever we used is a commercial PiezoleverTM self-sensing device. It is a 2KΩ piezo-resistive cantilever which is 305 μm long, 50 μm wide and 3 μm thick [Thermomicroscopes technical datasheet]. The cantilever's force constant is $k = 1 \text{ N/m}$ and its resonant frequency is 33 KHz. The tip extends about 2 μm from the cantilever. The tip was coated with a 60-nm-thick iron and magne-

tized along the tip axis, z , using a permanent magnet. The force gradient was around $4 \times 10^{-3} \text{ N/m}$ with small changes from one image to another.

III. RESULTS AND DISCUSSION

A. DC transport and magnetization

Figure 1 shows the resistivity and magnetization of a 150 Å film of LCMO on LAO and for comparison, the resistivity of a 150 Å film of LCMO on NGO. This figure summarizes the effect of lattice mismatch strain on the transport and magnetic properties. The film of LCMO on LAO is insulating but a metallic temperature dependence appears in an applied field of 8.5 T whereas a film of the same thickness on the lattice matched substrate NGO shows a resistivity behavior very close to that of bulk LCMO [12]. The magnetization (M) starts rising around 250 K but this rise is much slower than what is observed in thicker films of LCMO on LAO [12]. The inset shows the M vs. H curve for the film on LAO at 5 K. The saturation value of M (M_{sat}) is $\sim 1.8 \mu_B$ which is about 50 % of the expected $M_{sat} = 3.67 \mu_B$.

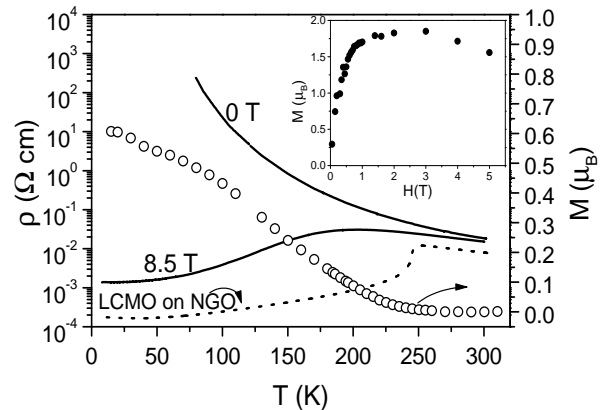


FIG. 1. A summary of the transport and magnetic properties of the 150 Å film of LCMO on LAO. The resistivity behavior of the film of LCMO on NGO in zero field is shown for comparison. In zero field the film on LAO is insulating at low temperatures. In a field of 8.5 T a metallic state appears at low temperature. The magnetization (taken in a field of 1000 G) shows a gradual rise as the temperature is lowered below $\sim 250 \text{ K}$. The inset shows that the film on LAO has a reduced saturation magnetization of $\sim 1.8 \mu_B$ at 5 K.

From these data we conclude that in zero field most of the volume of the film on LAO is in an insulating state, and the application of an 8.5 T field converts a sufficient volume fraction to a metallic state to allow metallic conduction. The magnetization data shows that the M_{sat} is about half of what is expected. This could be due to: (1) Spin-canting and the out-of-plane orientation of the spins resulting from the strained growth and (2) phase

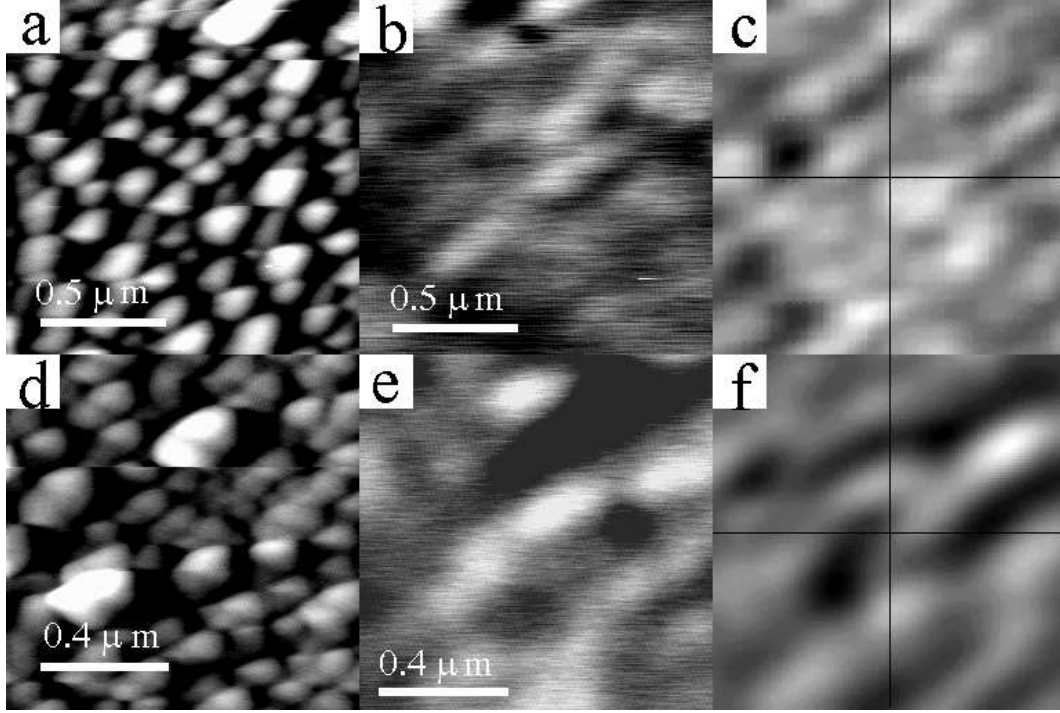


FIG. 2. MFM images taken at 80 K of the film of LCMO on LAO. The images (a) and (d) are topographic images, which are $1.4 \mu\text{m} \times 1.4 \mu\text{m}$ and $1.1 \mu\text{m} \times 1.1 \mu\text{m}$ respectively. (b) and (e) are the corresponding magnetic images of the same area. (c) and (f) are the cross correlation functions of the corresponding topographic and magnetic images. The axes for the displacements in the x and y directions are marked. The areas of the cross correlation images are the same as their respective scan areas. Note the shifts of the regions of maximum correlation (brighter regions) from the origin in (c) and (f) (the center of the image is the origin).

separation into FMM and COI phases. Since, from the transport data it is clear that in zero field a large volume fraction of the film is in the insulating state [we will argue in following sections that it is a charge-ordered insulating state] which in manganites is a non-ferromagnetic state, we claim that the reduction in the M_{sat} is mainly due to the phase separation into ferromagnetic and non-ferromagnetic phases. In the following sections magnetotransport and MFM measurements will strengthen this claim and we will discuss the nature of these two phases.

In an earlier paper we showed using atomic force microscopy and cross sectional high resolution transmission electron microscopy results that under compressive strain the film grows in the form of islands and the strain was distributed non-uniformly through the sample [6]. From these observations we propose the following hypothesis. The origin of the two-phase behavior is the non-uniform strain produced in the compressively strained film due to the island growth mode [6,13]. The initial layers of the film grow coherently with the substrate and are therefore under uniform compressive stress. After a certain thickness the 3D-islands are nucleated. The edges of these islands are regions of high strain while the top of the islands are regions of low strain. Since, from the magnetization data, it is clear that the low temperature phase is ferromagnetic albeit with a reduced magnetic moment,

it was suggested in ref. [6] that the top of the 3D islands are regions of low strain and are FMM at low temperatures. These FMM regions are separated by the high strain regions at the edges of the islands which are in the COI phase due to the strain induced lattice distortion. In contrast, the lattice matched film on NGO grows in the step flow mode and even 150 \AA films of LCMO display the properties shown by bulk LCMO and there is no suggestion of a two-phase behavior [6]. In the remainder of this paper we will present strong evidence in support of this hypothesis and discuss in detail the reasons and implications.

B. Low temperature MFM measurements

To confirm the hypothesis mentioned above, we first obtained images of the magnetic domain structure in the films of LCMO on LAO (which shows the island growth mode) and LCMO on NGO (which shows the step flow growth mode) using a low temperature MFM. Although a calibration of the actual local field and its gradient is difficult from an MFM measurement, we can get important information about the magnetic structure of the films at a scale of $\sim 500 \text{ \AA}$. Figure 2 shows the MFM images of the films of LCMO on LAO. Figure 2a and 2b are

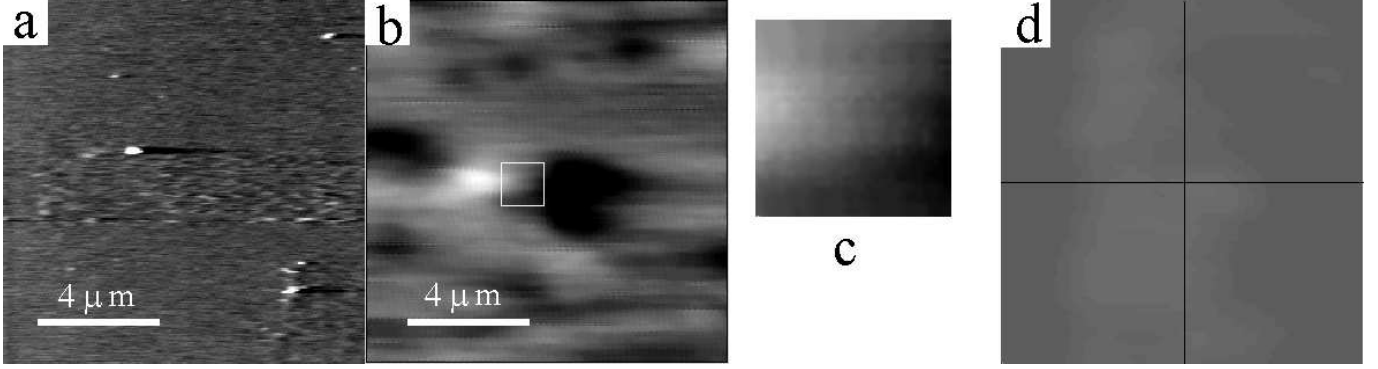


FIG. 3. (a) Topographic and (b) magnetic images of an LCMO film on NGO taken at 80 K. The scan area is $12\ \mu\text{m} \times 12\ \mu\text{m}$. The square marks an area of $1.4\ \mu\text{m} \times 1.4\ \mu\text{m}$ which is shown magnified in (c). The domain sizes are much larger than for the film on LAO. (d) shows the cross-correlation of the topographic and magnetic images and has the same area as the scan size. The featurelessness of the cross correlation shows that the magnetic structure for this film grown under negligible strain is uncorrelated to the topography.

topography and magnetic images respectively, taken over the same area and figure 2d and 2e are topography and magnetic images taken over another area. First we make some qualitative comments about the images. The magnetic images clearly shows the presence of ferromagnetic (FM) regions in the film on LAO which shows that at low temperatures a significant part of the film is in the FMM state although the film is insulating down to the lowest temperatures. Also, the domain sizes are of the same order as the island sizes. To analyze the images quantitatively, in figure 2c and 2f we show the 2D cross correlation images of the topographic and magnetic images. 2D cross correlation is the usual method for 2D pattern recognition. The cross correlation images have their origin (zero displacement) at the center of the image and their areas are the same as the corresponding topographic and magnetic images. The positions of high correlation in the images (brighter regions) mark the relative displacements at which the topography and the magnetic images are highly correlated. From figure 2c and 2f we can see that there is a high correlation between the topography and magnetic images which, for one, shows that the magnetism of the film is linked to the topography. It also shows that the maximum correlation occurs at points slightly offset from the origin. Which means that the highest correlation between figures 2a and 2b and figures 2d and 2e happens when the topography and magnetic images are displaced relative to each other. This is understandable since the MFM image picks up the magnetic force gradient which is maximum at the edges of the islands [the change in magnetization is expected to be maximum at the edges of the islands since the strain changes rapidly at these locations]. The maxima in the cross correlation are hence shifted from the origin by a distance of the order of the average island size. The images of the film on NGO are shown for comparison in figure 3. The domain sizes are much larger ($\sim 5 - 10\ \mu\text{m}$) than the film on LAO. This is the typical

domain size observed in the FMM state of manganites [7]. There is no correlation between the topography and the magnetism of the film as seen in figure 3d.

Although these results are limited by the resolution of the MFM and the fact that we cannot get a direct measure of the actual local field, the results shown above lend strong support to our claim that the magnetic and topographic structure of the film on LAO are linked to each other. This is due to the variation of the local strain in the film growing under compressive strain in the form of islands. The non-uniform strain results in the coexistence of FM regions (in the areas of low strain) and non-FM regions (in the areas of high strain). In the next subsection we discuss the properties of the non-FM regions in detail.

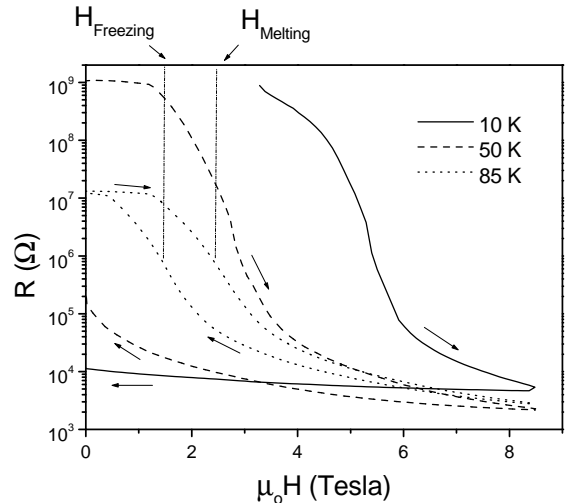


FIG. 4. R vs. H curves for the film of LCMO on LAO for three temperatures. The melting and freezing fields are marked.

C. The $T - H$ phase diagram

Two points are confirmed by the discussion above, 1) the local magnetism of the non-uniformly strained LCMO film on LAO is linked to the microstructure and hence to the distribution of strain and 2) the film has a significant portion of FM regions at low temperature, which accounts for the magnetic moment of $\sim 1.8\mu_B$ observed at low temperatures. Yet the film is insulating and has a large MR at low temperatures which is due to the non-FM regions mentioned earlier. We now investigate this insulating state further.

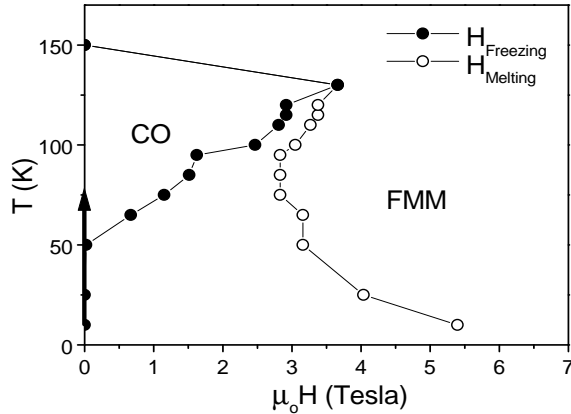


FIG. 5. The $T - H$ phase diagram of the film of LCMO on LAO. The phase diagram closely resembles that for $\text{Pr}_{1-x}\text{Ca}_x\text{MnO}_3$ ($x \sim 0.33$). The arrow on the y-axis shows the path in the phase diagram which was followed to get the R vs. T curve shown in figure 6.

Figure 4 shows the ρ vs. H behavior of the film at low temperatures. In each case the sample was zero field cooled to that particular temperature. The magnetic field was then increased and then reduced to zero. It shows that there is a sharp transition to a low resistance state above a certain magnetic field and this transition is associated with a significant hysteresis. This behavior is similar to the phenomenon of melting of a charge ordered state by a magnetic field which is a first order transition and is associated with a large temperature dependent hysteresis [14]. A set of R vs. H curves taken at different temperatures has been used to construct a phase diagram in the $T - H$ plane. Such a phase diagram for the 150 Å film on LAO is shown in figure 5. H_{Freezing} and H_{Melting} were determined from the R vs. H curves as the field values at which dR/dH was maximum (Fig. 4). These data show that the insulating state at low temperatures displays a behavior just like bulk compounds in the charge ordered state [14,15]. Note that in bulk $\text{La}_{0.67}\text{Ca}_{0.33}\text{MnO}_3$ there is no charge ordered state at low temperature but a low temperature FMM state. Therefore we conclude that the regions of high strain (near the edges of the islands) have a distortion built into the lattice structure due to the sub-

strate induced strain which leads to the destabilization of the FMM state at low temperatures and the charge ordered state takes over. Furthermore, the phase diagram shows that for $T < 50\text{K}$ the insulating state does not recover even when the field is reduced to zero. Such behavior is similar to that observed in compounds with $\langle r_A \rangle \leq 1.18 \text{ Å}$ such as $\text{Pr}_{1-x}\text{Ca}_x\text{MnO}_3$. It has been shown for uniformly strained films that by tuning the c/a ratio, the magnetic and electronic phases can be controlled [16]. The data for thin films of $\text{La}_{1-x}\text{Sr}_x\text{MnO}_3$ grown on different substrates with different amounts of strain (and hence different c/a ratios) were compared to the data for $\text{Nd}_{1-x}\text{Sr}_x\text{MnO}_3$ for different x (which varies the c/a ratio in this case). In our films we have shown that the strain is non-uniform due to the island like growth mode which suggests that the c/a ratio varies over the film. The average c/a ratio is ~ 1.04 (as determined from the lattice constant measurements) but from the MFM and magnetization results it is clear that some parts of the film (the top of the islands) are relatively strain free i.e. $c/a \approx 1$. The LCMO film on LAO has therefore been distorted locally resulting in a variation of the c/a ratio over the film and hence a variation of the magnetic and electronic properties.

It has been shown by Dörr *et al.* that in oxygen deficient films of LCMO a phase separation between FMM and an antiferromagnetic insulating phase is observed [17]. This is due to reduced Mn^{4+} concentration in the sample. Even in our samples oxygen annealing of the film on LAO results in the film becoming FMM at low temperatures [6]. However, we argue in the following that the two-phase behavior we observe is strain driven and not due to variations in stoichiometry and the oxygen annealing results mainly in a reduction of this strain. The basis for our argument is the $T - H$ phase diagram in fig. 5. In the bulk $\text{La}_{1-x}\text{Ca}_x\text{MnO}_3$, there is no value of x for which there is such a $T - H$ phase diagram. The most striking evidence is the fact that at 10 K there is a drop of about 5 orders of magnitude in the resistance at a field of about 6 T and the insulating state is not recovered when the field is removed (fig. 4). Also for the CO state seen for $x \geq 0.5$ in bulk $\text{La}_{1-x}\text{Ca}_x\text{MnO}_3$, the melting fields are about 14 T and higher [18,19]. Therefore, this strain driven phase of LCMO cannot be explained as being due to a variation in stoichiometry. In fact this state is similar to the charge ordered state in the $\text{Pr}_{1-x}\text{Ca}_x\text{MnO}_3$ system for $x \sim 0.3$, as can be seen from the phase diagram in figure 5 [15]. Therefore this two-phase state comprising FMM and COI regions obtained by applying biaxial strain is a new, strain driven, state of LCMO. We are further investigating the additional role of oxygen deficiency on such a strain driven COI state by systematically reducing the oxygen content of our films on LAO.

D. Metastable states and long time scale dynamics

From figure 5 we observe that the width of the hysteresis in the R vs. H curves increases as the temperature is lowered. This is due to the decrease of the effect of thermal fluctuations on the first order transition [14]. As mentioned earlier, for $T < 50$ K the metallic state obtained on melting the CO state by a magnetic field is retained even after the magnetic field is removed. This is a metastable state and the high resistance state is recovered when the temperature is raised above 50 K

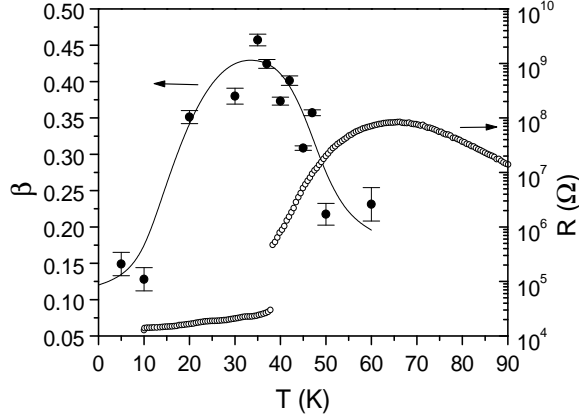


FIG. 6. The values of β as a function of temperature. The solid line is a guide to the eye. The behavior of the resistance along the path marked in figure 5 is also shown. There is large jump in the resistance around 40 K and the insulating state is recovered near 65 K.

as shown in figure 6. This association of the two-phase coexistence with the local structural distortions results in slow dynamics which we have measured as the slow relaxation of the resistance of a metastable state. We obtained the metastable state as follows. We first cooled down the sample in zero field and applied a magnetic field of 8.5 T at 5 K. A metallic state was thus obtained. The field was then removed but the film was still trapped in the metastable metallic state. We then measured the resistance as function of time of this metastable state. The resistance increases as a function of time. The relaxation of the resistance can be fitted with a stretched exponential form $R(t) = R_0 - R_1 \exp[-(t/\tau)^\beta]$. The stretched exponential form of the relaxation has been observed in numerous systems but the exact physical significance of the fit parameters β and τ is not fully understood. In particular, such long time scale relaxation of the resistance has been observed in bulk charge-ordered systems like $\text{La}_{0.5}\text{Ca}_{0.5}\text{MnO}_3$ and $\text{La}_{5/8-y}\text{Pr}_y\text{Ca}_{3/8}\text{MnO}_3$ [20,21]. One conclusion which can be drawn from these observations is that there are metastable states which are separated by energy barriers with a wide distribution of energies which leads to a distribution of relaxation times and the stretched exponential form of relaxation. The time constant τ has been observed to be thermally acti-

vated i.e. of the form $\tau = \tau_0 \exp(E_\tau/k_B T)$. E_τ is related to the distribution of physical activation energies [22]. A variation of E_τ suggests that the activation energies in the system have been changed. For the film of LCMO on the LAO, $E_\tau \sim 96 \pm 5$ K (figure 7). It is interesting to compare the value of E_τ with the field required to melt the charge ordered state at low temperatures (H_{M0}). Ref. [21] gives the values of E_τ for the two compounds $\text{La}_{0.5}\text{Ca}_{0.5}\text{MnO}_3$ and $\text{La}_{5/8-y}\text{Pr}_y\text{Ca}_{3/8}\text{MnO}_3$ ($y = 0.375$). The inset of figure 7 shows a plot of E_τ vs. H_{M0} which shows that the two are linearly related. This analysis of the slow relaxation of the resistance shows that the strength of the charge ordered state depends on the distribution of activation energies between the metastable

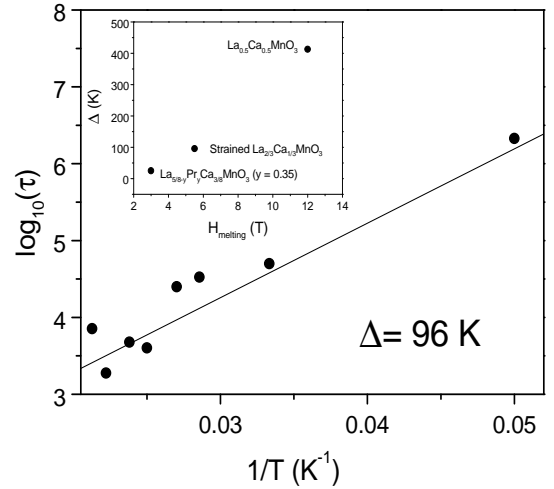


FIG. 7. The $1/T$ vs. $\log \tau$ plot. The value of E_τ is 96 ± 5 K. The inset shows a plot of E_τ vs. $H_{melting}$ for three materials. The first and third points are taken from ref. 21.

states. This could presumably be due to the activation energy barriers being associated with motion of domain walls in the phase separated regime, which suggests that the field driven transition is perhaps not a thermodynamic transition. The physical significance of the value of β is less clear. The only comment which can be made is that near the temperature where the metastable, low resistance state makes the transition to the higher resistance state, the β value reaches up to ~ 0.5 . This indicates that the distribution of the energies of the barriers is the broadest near the transition [22]. Similar values of β ($0.34 < \beta < 0.46$) were also obtained from relaxation measurements in $\text{La}_{5/8-y}\text{Pr}_y\text{Ca}_{3/8}\text{MnO}_3$ ($y = 0.375$) [21].

IV. SUMMARY

In this paper we have shown that: (1) Film growth under biaxial compressive strain readily leads to a 3D island

growth mode which leads to a non-uniform distribution of the strain. This leads to pockets of high distortion (near the edges of the islands) and regions where the strain is very low (top of the islands). (2) For a system like $\text{La}_{0.67}\text{Ca}_{0.33}\text{MnO}_3$ which is cubic at low temperatures, the non-uniform strain leads to the ratio $c/a \neq 1$ in the high strain regions and $c/a \sim 1$ in the low strain regions. (3) The low strain regions are FM at low temperatures and contribute to the saturation magnetization of $1.8 \mu_B$. (4) The high strain regions are in the CO state at low temperatures and result in the insulating behavior of the film in zero field. The magnetoresistance behavior of the film shows that the strain drives the LCMO film to a state similar to the low temperature state observed in $\text{Pr}_{1-x}\text{Ca}_x\text{MnO}_3$ ($x \sim 0.33$). (5) The two-phase behavior of the film is coupled to the localized structural distortions and this leads to slow dynamics in the transport properties of the film. There is a distribution of the activation energies separating the metastable states and this distribution of energies determines the strength of the COI state. It has been shown in [23] that there is a strong coupling between the lattice, Mn e_g orbital state, and the exchange interaction. When we perturb the lattice by the non-uniform strain it results in inhomogeneities in the exchange and hopping interactions. Near first order transitions such disorder leads to large scale two-phase coexistence [24]. This disorder can also be introduced by chemical substitution [21]. Disorder is therefore an essential ingredient for the occurrence of large scale phase separation.

V. CONCLUSIONS

The most important claim that we make is that there is a strain driven COI state in $\text{La}_{0.67}\text{Ca}_{0.33}\text{MnO}_3$ which is similar to the small $< r_A >$ compound $\text{Pr}_{0.67}\text{Ca}_{0.33}\text{MnO}_3$. We support this claim with MFM and magnetotransport data. These are not “confirmatory tests” for detection of a charge ordered state like electron diffraction [3]. We are still trying to devise a method to do perform such a confirmatory test on these samples. Nevertheless, in this paper we have presented compelling evidence to support our claims.

The results shown above elucidate the instability of the FMM(COI) phases towards the COI(FMM) phases on the application of perturbation like a magnetic field, external or internal stress etc. At certain values of these external parameters there are first order transitions between these two phases. Near these first order transitions, the defects in the sample stabilize the observed large scale phase separation in hole-doped manganites. Such effects are therefore intrinsic to the behavior of manganites and have to be accounted for when explanations of the properties of manganites are attempted.

ACKNOWLEDGMENTS

This work was partially supported by the MRSEC program of the NSF at the University of Maryland, College Park (Grant No. DMR-0080008).

-
- [1] J. P. Attfield, Chem. Mater. **10**, 3239 (1998) and references therein
 - [2] P. V. Vanitha, P. N. Santhosh, R. S. Singh, C. N. R. Rao, and J. P. Attfield, Phys. Rev. B **59** 13539 (1999)
 - [3] M. Uehara, S. Mori, C. H. Chen, and S.-W. Cheong, Nature **399**, 560 (1999)
 - [4] M. Fäth, S. Freisem, A. A. Menovsky, Y. Tomioka, J. Aarts and J. A. Mydosh, Science **285** 1540 (1999)
 - [5] H. S. Wang, Qi Li, Kai Liu and C. L. Chien, Appl. Phys. Lett. **74**, 2212 (1999), J. Z. Sun, D. W. Abraham, R. A. Rao, and C. B. Eom, Appl. Phys. Lett. **74** 3017 (1999)
 - [6] Amlan Biswas, M. Rajeswari, R. C. Srivastava, Y. H. Li, T. Venkatesan, R. L. Greene and A. J. Millis, Phys. Rev. B **61**, 9665 (2000)
 - [7] C. W. Yuan, E. Batalla, A. de Lozanne, M. Kirk, M. Tortonese, Appl. Phys. Lett. **65**, 1308 (1994)
 - [8] C. W. Yuan, Z. Zheng, A. L. de Lozanne, M. Tortonese, D. A. Rudman, J. N. Eckstein, J. Vac. Sci. Technol. B **14**, 1210 (1996)
 - [9] Chun-Che Chen, Qingyou Lu, Caiwen Yuan, Alex de Lozanne, James N. Eckstein, and Marco Tortonese, in Proc. of the 10th Anniversary HTS Workshop on Physics, Materials and Applications, ed. by B. Batlogg, C.W. Chu, W.K. Chu, D.U. Gubser and K.A. Müller (World Scientific, Singapore, 1996) pg.599.
 - [10] Q. Lu, C. -C. Chen, and A. L. de Lozanne, Science **276**, 2006 (1997)
 - [11] Chun-Che Chen, Qingyou Lu, Alex de Lozanne, Appl. Phys. A **66**, S1181 (1998).
 - [12] M. Jaime, P. Lin, S. H. Chun, M. B. Salamon, P. Dorsey and M. Rubinstein, Phys. Rev. B **60**, 1028 (1999)
 - [13] Y. Chen and J. Washburn, Phys. Rev. Lett. **77**, 4046 (1996)
 - [14] H. Kuwahara, Y. Tomioka, A. Asamitsu, Y. Moritomo, and Y. Tokura, Science **270**, 961 (1995).
 - [15] Y. Tomioka, A. Asamitsu, H. Kuwahara, Y. Moritomo, and Y. Tokura, Phys. Rev. B, **53**, R1689 (1996)
 - [16] Y. Konishi *et al.*, J. Phys. Soc. Jpn., **68**, 3790 (1999)
 - [17] K. Dörr *et al.*, J. Phys.: Condens. Matter, **12**, 7099 (2000)
 - [18] Gang Xiao *et al.*, J. Appl. Phys. **81**, 5324 (1997)
 - [19] S. -W. Cheong and C. H. Chen, in *Colossal Magnetoresistance, Charge Ordering and Related Properties of Manganese Oxides*, edited by C. N. R. Rao and B. Raveau (World Scientific, Singapore, 1998), pp. 241-278
 - [20] V. N. Smolyaninova, C. R. Galley and R. L. Greene, cond-mat/9907087
 - [21] M. Uehara *et al.*, (to be published)

- [22] L. E. Benatar, D. Redfield, and R. H. Bube, J. Appl. Phys. **73**, 8659 (1993)
- [23] K. H. Ahn and A. J. Millis, cond-mat/0004295
- [24] A. Moreo, M. Mayr, A. Feiguin, S. Yunoki, and E. Dagotto, Phys. Rev. Lett. **84**, 5568 (2000)